materials

MDPI

Article

A New Strategy to Improve the Toughness of Epoxy Thermosets—By Introducing Poly(ether nitrile ketone)s Containing Phthalazinone Structures

Hongjun Guo [1,2,3], Bing Wang [1,2,4], Xin Fu [5], Nan Li [1,2,*], Guiyang Li [3], Guodong Zheng [3], Zaiyu Wang [6], Cheng Liu [1,2], Yousi Chen [1,2], Zhihuan Weng [1,2], Shouhai Zhang [1,2] and Xigao Jian [1,2,4,*]

1 State Key Laboratory of Fine Chemicals, Frontier Science Center for Smart Materials, Dalian University of Technology, Dalian 116024, China
2 Technology Innovation Center of High Performance Resin Materials, Dalian 116024, China
3 Aerospace Research Institute of Materials & Processing Technology, Beijing 100076, China
4 School of Materials Science and Engineering, Dalian University of Technology, Dalian 116024, China
5 Wuhan Second Ship Design and Research Institute, Wuhan 430064, China
6 AVIC Jiangxi Hongdu Aviation Industry Group Company Ltd., Nanchang 330024, China
* Correspondence: polymerlinan@dlut.edu.cn (N.L.); jian4616@dlut.edu.cn (X.J.)

Abstract: As high brittleness limits the application of all epoxy resins (EP), here, it can be modified by high-performance thermoplastic poly(ether nitrile ketone) containing phthalazinone structures (PPENK). Therefore, the influence of different PPENK contents on the mechanical, thermal, and low-temperature properties of EP was comprehensively investigated in this paper. The binary blend of PPENK/EP exhibited excellent properties due to homogeneous mixing and good interaction. The presence of PPENK significantly improved the mechanical properties of EP, showing 131.0%, 14.2%, and 10.0% increases in impact, tensile, and flexural strength, respectively. Morphological studies revealed that the crack deflection and bridging in PPENK were the main toughening mechanism in the blend systems. In addition, the PPENK/EP blends showed excellent thermal and low-temperature properties (−183 °C). The glass transition temperatures of the PPENK/EP blends were enhanced by approximately 50 °C. The 15 phr of the PPENK/EP blends had a low-temperature flexural strength of up to 230 MPa, which was 46.5% higher than EP. Furthermore, all blends exhibited better thermal stability.

Keywords: PPENK; epoxy resin; toughness and strength; low-temperature properties

Citation: Guo, H.; Wang, B.; Fu, X.; Li, N.; Li, G.; Zheng, G.; Wang, Z.; Liu, C.; Chen, Y.; Weng, Z.; et al. A New Strategy to Improve the Toughness of Epoxy Thermosets—By Introducing Poly(ether nitrile ketone)s Containing Phthalazinone Structures. *Materials* **2023**, *16*, 2878. https://doi.org/10.3390/ma16072878

Academic Editor: Andrea Sorrentino

Received: 1 March 2023
Revised: 21 March 2023
Accepted: 29 March 2023
Published: 4 April 2023

Copyright: © 2023 by the authors. Licensee MDPI, Basel, Switzerland. This article is an open access article distributed under the terms and conditions of the Creative Commons Attribution (CC BY) license (https://creativecommons.org/licenses/by/4.0/).

1. Introduction

Epoxy resins are widely used in aerospace, vehicles, ships, coatings, electronic materials, and other fields due to their excellent chemical stability, heat resistance, dimensional stability, and good processing properties [1–3]. However, due to a large number of reactive groups in epoxy resin, it shows shortcomings such as high cross-linking density, sizeable internal stress, brittleness, poor toughness, easy cracking, and poor impact resistance after curing [4]. This limits its wide applications in structural adhesives, wind power blades, electronic and electrical packaging materials, and high-performance composites for aerospace. Therefore, modifying epoxy resin, especially improving its toughness, has always been an important research direction for researchers [5].

Researchers have extensively studied the toughening modification of epoxy resin in the past few decades, and there are mainly two types of methods. One is introducing a "flexible segment" [6,7]. By modifying the curing agent or epoxy resin, the "flexible segment" enters, thereby improving the resin molecular chain's flexibility, fluidity, and toughness. However, it significantly reduces the strength and modulus of the material [8,9]. Another strategy is incorporating secondary components such as rubbers [10,11], nanoparticles [12–14], the thermotropic liquid crystalline polymer [15–17], and thermoplastic resins [18–21] into epoxy resins. Unfortunately, adding rubber particles can significantly reduce the system's modulus

and glass transition temperature [22], and the uneven distribution of nanoparticles can lead to defects in the material [23]. In addition, the high cost and high processing temperature of thermotropic liquid crystals also limit their application in toughening modification.

In recent years, toughening and modification of epoxy resins using high-strength, high-toughness, high-heat-resistance thermoplastic resins have attracted the extensive attention of researchers [24,25]. Karthikeyan et al. [26] introduced hydroxyl-functionalized poly (ether ether ketone) (PEEK) into glycidyl ether of bisphenol A (DGEBA) epoxy resin, which improved its maximum lap shear strength and fracture toughness. Rehman et al. [27] investigated the effect of micro-PEEK particles on the damage response of carbon/epoxy composites under the low-velocity impact. They showed that introducing PEEK particles improved the toughness and damage tolerance of carbon/epoxy composites. Gresil et al. [4] used polyethersulfone (PESU) to modify epoxy anhydride thermosetting plastics and investigated its effect on the morphological, thermal, and mechanical properties of epoxy resins. Although the above thermoplastic resins enhanced the toughness of the epoxy resin, there was no significant improvement in its toughness due to their poor compatibility.

Poly(phthalazinone ether nitrile ketone)s (PPENK, Figure 1), as a new type of high-performance engineering plastic, has excellent mechanical and thermal properties (glass transition temperature ≥ 240 °C) [28]. At the same time, it has a fully aromatic ring twisted non-coplanar molecular structure, giving it solubility. It can be hot-melt mixed with epoxy resin to improve its toughness and thermal properties.

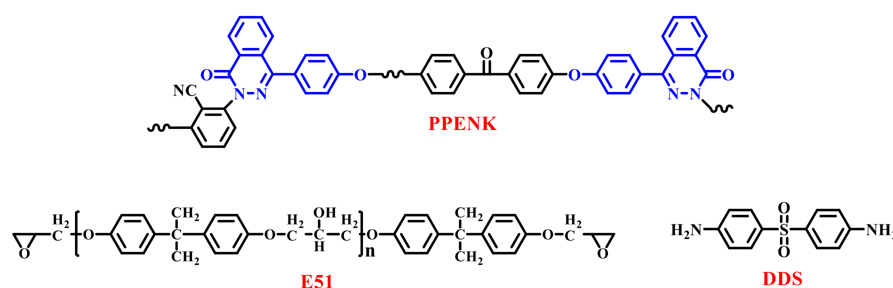

Figure 1. The molecular structure for PPENK, E51, and DDS.

Herein, we used the PPENK-containing phthalazinone structure to toughen epoxy resin. PPENK was hot-melt mixed with epoxy resin to prepare a series of epoxy blends with different contents of PPENK. The effects of PPENK content on the blends' thermal properties, mechanical properties, and low-temperature properties were investigated. Therefore, this research is expected to open a new avenue for improving epoxy resin's mechanical, thermal, and low-temperature properties using high-performance thermoplastic polymers.

2. Experiment

2.1. Materials and Methods

E51 epoxy (Figure 1) resin from Shenyang Haotian Resin Material Co., Ltd. (Shenyang, China), PPENK (Nitrile/Ketone, 1/1; Mn, 29,125 g/mol; density, 1.26 g/cm^3; intrinsic viscosity, 0.46 dL/g) from Chengdu Tianshun Polymer New Material Co., Ltd., Liaoning, China, 4,4′-diaminodiphenyl sulfone (DDS, Figure 1) from Shanghai Maclean Biochemical Technology Co., Ltd. (Shanghai, China).

This study used the hot-melt mixed method to prepare the PPENK/E51 blends. The quality content of PPENK in the blend was 3, 5, 10, 15, and 20 phr (Parts per hundred parts of resin). The following is a brief description of the 10 phr sample.

A mass of 200 g of E51 and 10 g of PPENK were added to a three-necked flask, heated to 130 °C, and mixed for 1–2 h. A mass of 60 g of curing agent DDS was added, the solution was stirred well, and the hot mixture was poured into the mold (Figure S6) and placed in a vacuum oven to remove air bubbles. Then cured (procedure: 120 °C/2 h + 150 °C/1 h + 190 °C/2 h + 220 °C/2 h).

2.2. Instrumentation and Methods

DSC 204 instrument tested the curing behavior of the uncured samples (5–10 mg) at different heating rates (β = 5, 10, 15, 20 °C/min) from 30 °C to 350 °C; and on blends (5–10 mg) to determine the glass transition temperature (T_g) at a heating rate of 10 °C/min with a 3-stage ramp-up procedure: 30–250 °C, 250–30 °C, 30–250 °C. Additionally, the curing behavior of uncured samples (5–10 mg) was tested at a heating rate of 10 °C/min from 30 °C to 350 °C, and all tests were performed under an N_2 atmosphere with a flow rate of 50 mL/min.

FT-IR spectra of the blends were obtained on a Nicolet-20DXB infrared spectrometer with the single reflection ATR method (range: 500 cm^{-1} to 4000 cm^{-1}).

Mettler TGA/SDTA851 analyzer was used to test the thermal decomposition temperatures of the blends (5–10 mg) from 30 °C to 800 °C under N_2 atmosphere (N_2 flow rate of 50 mL/min) at a ramp rate of 20 °C/min.

The scanning electron microscope (SU8220 and FlexSEM 1000) was used to record the SEM images of the blend.

According to the ASTM D4812-99, the impact strength of non-notched samples with a dimension of 80 × 10 × 4 mm^3 was measured from the XCJ-4 type Charpy machine, with at least 5 samples per group measured.

According to the ASTM D790-17, the flexural properties of samples with a dimension of 80 × 10 × 4 mm^3 were tested by the Instron 5869 machine, with at least 5 samples per group measured.

According to the ASTM D638-22, the tensile properties of the samples with a dimension of 115 × 10 × 4 mm^3 (dumbbell shape) were tested by the Instron 5869 machine, with at least 5 samples per group measured.

According to the ASTM D790-17, the samples' low temperatures (−183 °C) flexural properties with a dimension of 80 × 10 × 4 mm^3 were tested by the SDS-100 machine fitted with a thermodynamic environmental chamber, with no less than 5 samples per group.

According to the ASTM D638-22, the low temperatures (−183 °C) tensile properties of the samples with a dimension of 115 × 10 × 4 mm^3 (dumbbell shape) were tested by the SDS-100 machine fitted with a thermodynamic environmental chamber, with at least 5 samples per group measured.

TA Q800 dynamic mechanical analyzer (single cantilever mode, the frequency was 1 HZ) was used for testing the dynamic thermomechanical properties of 40 × 6 × 3 mm^3 rectangular samples at 5 °C/min from 35 °C to 250 °C.

3. Results and Discussion

3.1. Curing Behavior

The curing behavior of neat E51 and 10 phr-PPENK/E51 blend was investigated to demonstrate the effect of PPENK on E51 resin's curing kinetics. Figure 2A,B are the DSC curves of neat E51 and 10 phr-PPENK/E51 blends with different ramp rates, respectively. The heating curve of all systems exhibited a single and symmetrical feature. In addition, as the heating rate increased, the exothermic peak became higher and steeper. It shifted towards high temperatures direction, mainly due to the significant temperature difference in the system. The apparent activation energy (Ea) is one of the most important parameters for measuring the curing reaction activity of the systems [29]. It can usually be calculated by the Kissinger and the Flynn–Wall–Ozawa equations (Supplementary Material) [30], and the values of Ea are shown in Table 1. Ea of 10 phr-PPENK/E51 blends were slightly different from the pure E51, suggesting that PPENK had a smaller influence on the curing reaction of E51. In addition, Figure 2C shows the DSC curves (at a heating rate of 10 °C/min) for the different contents of PPENK blends. All curves showed only one exothermic peak, and PPENK did not increase the exothermic peak, indicating that temperature was decisive in the curing process and that the influence of PPENK content was small.

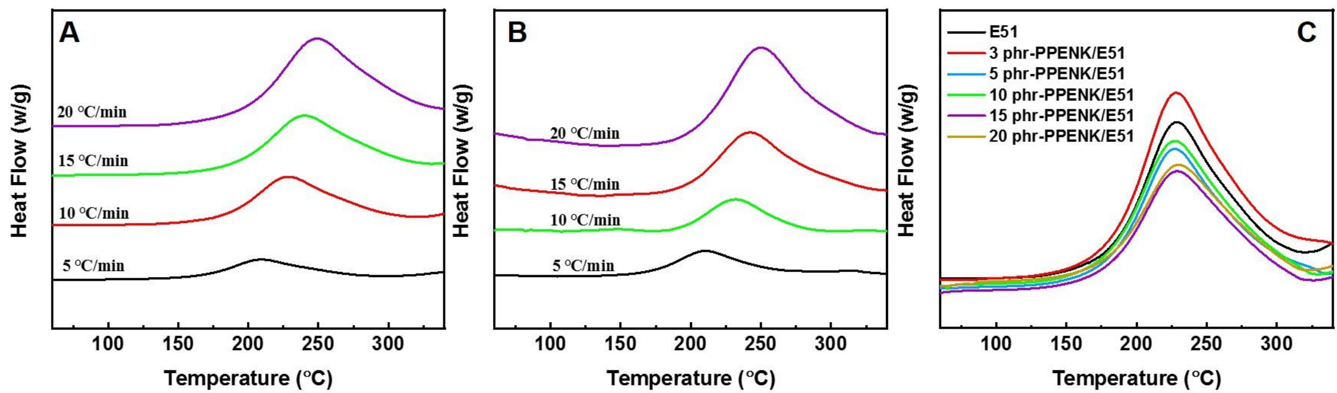

Figure 2. DSC curves: (**A**) E51 and (**B**) 10 phr-PPENK/ E51 (different heating rates), (**C**) PPENK/E51 blends with different content.

Table 1. The DSC dates of the different blends.

Blend Systems	Ea by Kissinger Equation (kJ/mol)	Ea by Ozawa Equation (kJ/mol)	Ea Average (kJ/mol)	$T_{i,\beta} = 0$ (°C)	$T_{top,\beta} = 0$ (°C)	$T_{f,\beta} = 0$ (°C)
E51/DDS	52.6	67.4	60.0	134	201	248
10 phr-PPENK/E51	50.4	65.4	57.9	129	200	241

3.2. FT-IR Analysis

To clarify the influence of PPENK on the chemical structure of cured E51 resin. FT-IR of 10 phr-PPENK/E51 was demonstrated in Figure 3. As seen in Figure 2, 906 cm^{-1} was the characteristic absorption peak of the epoxy group [31], and 3372 cm^{-1} and 3472 cm^{-1} were assigned to the characteristic peaks of N-H in the curing agent DDS. The above characteristic peaks disappeared completely after curing, indicating that the blends could be cured adequately under the curing procedure (120 °C/2 h + 150 °C/1 h+ 190 °C/2 h + 220 °C/2 h).

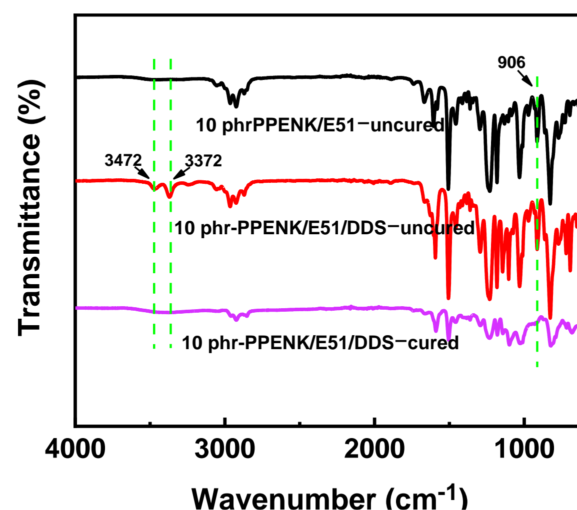

Figure 3. FTIR of 10 phr−PPENK/E51 blend with or without curing.

3.3. Glass Transition Temperatures (T_g)

DSC tested the T_g of blends with or without PPENK to determine the impact of PPENK on the thermal characteristics of E51. As shown in Figure 4, the T_g of the blends was significantly improved after the introduction of PPENK. The T_g of the PPENK/E51

blends were summarised in Table 2. On the one hand, PPENK had a higher T_g than E51 (see Table S4). Thus it would increase the T_g of the blend system. On the other hand, the introduction of PPENK caused a gradual decrease in the blend system's crosslink density (Table S3) [32], leading to the blend's T_g decrease. The combination of these two effects made the T_g of the blend system increase first and then decrease.

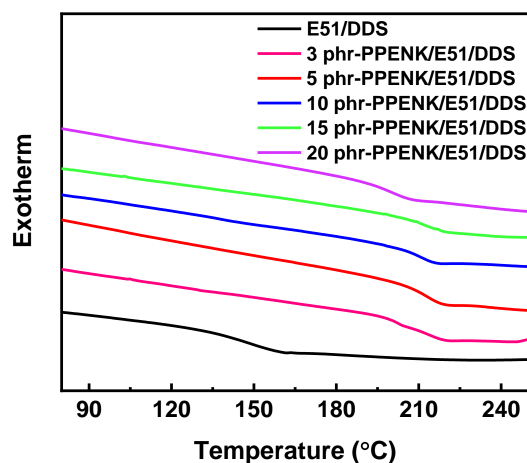

Figure 4. DSC curves of the blends with or without PPENK.

Table 2. The T_g and thermomechanical properties of blends.

Blend Systems	T_g (°C)		Initial-Er
	DSC	DMA	(GPa)
E51	154	166	3.27
3 phr-PPENK/E51	208	186	3.15
5 phr-PPENK/E51	214	188	3.00
10 phr-PPENK/E51	211	206	2.90
15 phr-PPENK/E51	213	201	2.88
20 phr-PPENK/E51	200	198	2.87

3.4. Thermomechanical Properties

The storage modulus (Er) and loss factor (Tanδ) of the cured E51 systems are depicted in Figure 5. From Figure 5, the storage modulus of the blends decreased slowly with increasing temperature, and the storage modulus decreased sharply when the temperature continued to increase, mainly due to the transition from the glass state of the system to the high elastic state. Interestingly, the initial-Er of the blends containing PPENK decreased compared with E51 due to a lower crosslink density of E51 after the addition of PPENK. On the one hand, the Er of the blend system mainly depended on the flexibility of the molecular segments [33]. The greater the flexibility, the lower the storage modulus. In the glass state, pure E51 had a large crosslink density, the molecular chain formed a network, and the flexibility of the molecular chain segment was poor, so the storage modulus was high [34]. After the introduction of PPENK, the PPENK/E51 blend's crosslink density decreased, and the flexibility of the molecular segments increased, resulting in a decrease in the initial Er. The effect of PPENK on the blend's crosslink density was explored using the theoretical equations of rubber elasticity (Supplementary material). The values of crosslink density are listed in Table S3. From Table S3, as PPENK content increased, the crosslink density of the blends gradually reduced; this was attributable to the dilution effect caused by adding PPENK, which decreased the density of reactive groups per unit volume, thereby reducing the crosslinking density [35,36].

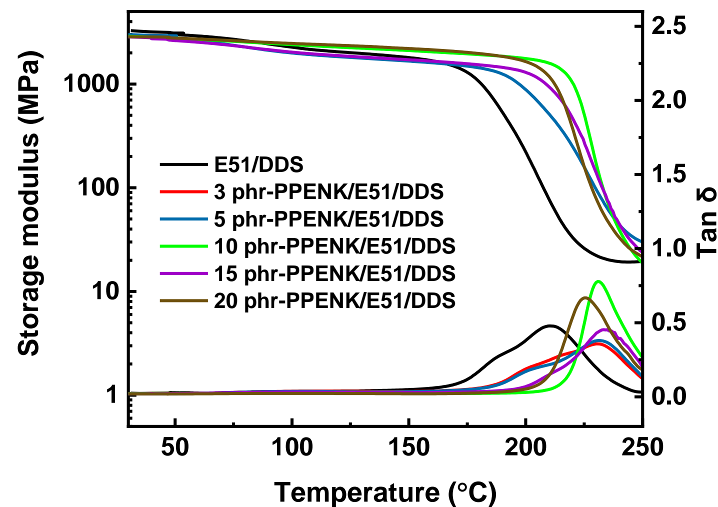

Figure 5. Thermomechanical properties of the blends.

The inflection point temperature of the polymer storage modulus curve was usually considered to be the T_g of the polymer. The T_g of the blended system with PPENK was significantly increased, similar to the DSC test results. In addition, there was only one loss peak in all blends, which indicated that the blend was a homogeneous system without interfacial separation.

3.5. Mechanical Properties

The mechanical properties of different proportions of PPENK/E51 blends are shown in Figure 6. As shown in Figure 6A, the impact strength of the blend system gradually increased as PPENK content was raised. When the content was 10 phr, the impact strength of the system reached a maximum of 37.0 kJ/m^2, which was about 131.0% higher than that of pure E51. When PPENK increased to 15 and 20 phr, the impact strength of the system decreased. In addition, as shown in Figure 5B,C, the changing trend of tensile and flexural strength was comparable to that of impact strength. When the content was 10 and 15 phr, the tensile and flexural strength reached the maximum value of 80 MPa and 133 MPa, respectively; this presented that PPENK could effectively increase the toughness and strength of E51 resin. For comparison, Table 3 shows some of the previous reports.

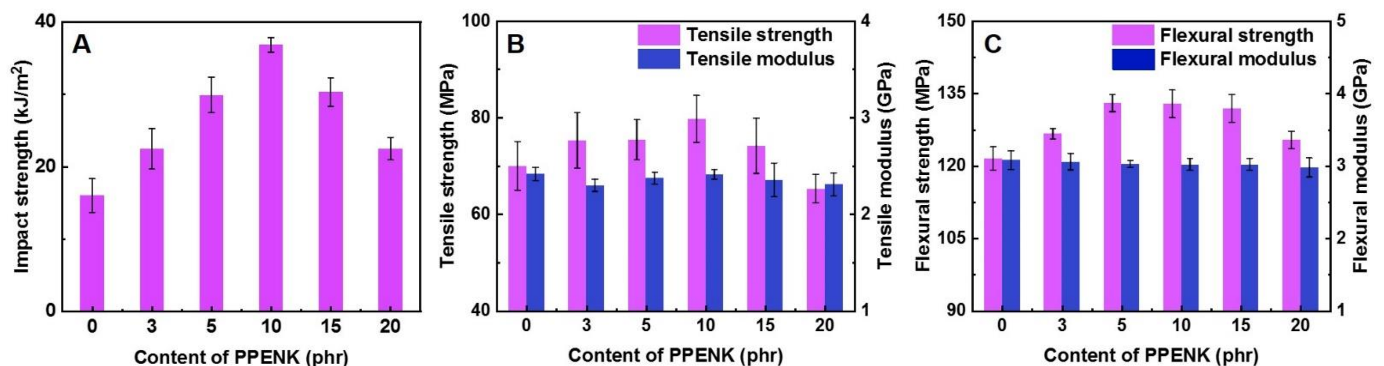

Figure 6. Mechanical properties of the blends: (**A**) Impact strength, (**B**) Tensile properties, (**C**) Flexural properties.

Table 3. Comparison of the toughening effect of PPENK/EP blend composites with the literature.

Blends	Content	Improvement Rate	Ref.
GO/PSF/EP	5.2 phr	89.9%	[14]
LCP/EP	10 phr	30%	[16]
DGE-DHBP/EP	10%	42.2%	[17]
PKHH/EP	10%	81.5%	[18]
PES/PEK−C/EP	15%	99.8%	[19]
PET/EP	4.8%	30.0%	[21]
PPENK/EP	10 phr	131.0%	This work

SEM observed the fracture surface after impact fracture to understand the toughening mechanism of PPENK−modified E51. From Figure 7A,B, pure E51 had a smooth fracture surface, the crack direction was single, and there was no apparent stress dispersion. On the contrary, after the introduction of PPENK in E51, the fracture morphology of the blend changed from smooth to relatively rough, and the cracks showed noticeable deflection and disproportionation. In addition, as shown in Figure 7H–L, there were many micro-cracks on the fracture surface, which increased the area of the fracture surface, and an apparent stress dispersion phenomenon occurred, which increased the fracture energy [37]. In addition, there were many polar groups (-CN) in the molecular chain of PPENK. These polar groups made a large number of interactions between PPENK and E51 [32]. When an external force damages the blend system, these weak interactions can withstand stress, consuming more crack propagation energy [38]. In addition, it has been reported in the literature that the blend system could exhibit a large amount of plastic deformation during the fracture process, thereby improving the toughness of the blend system [39].

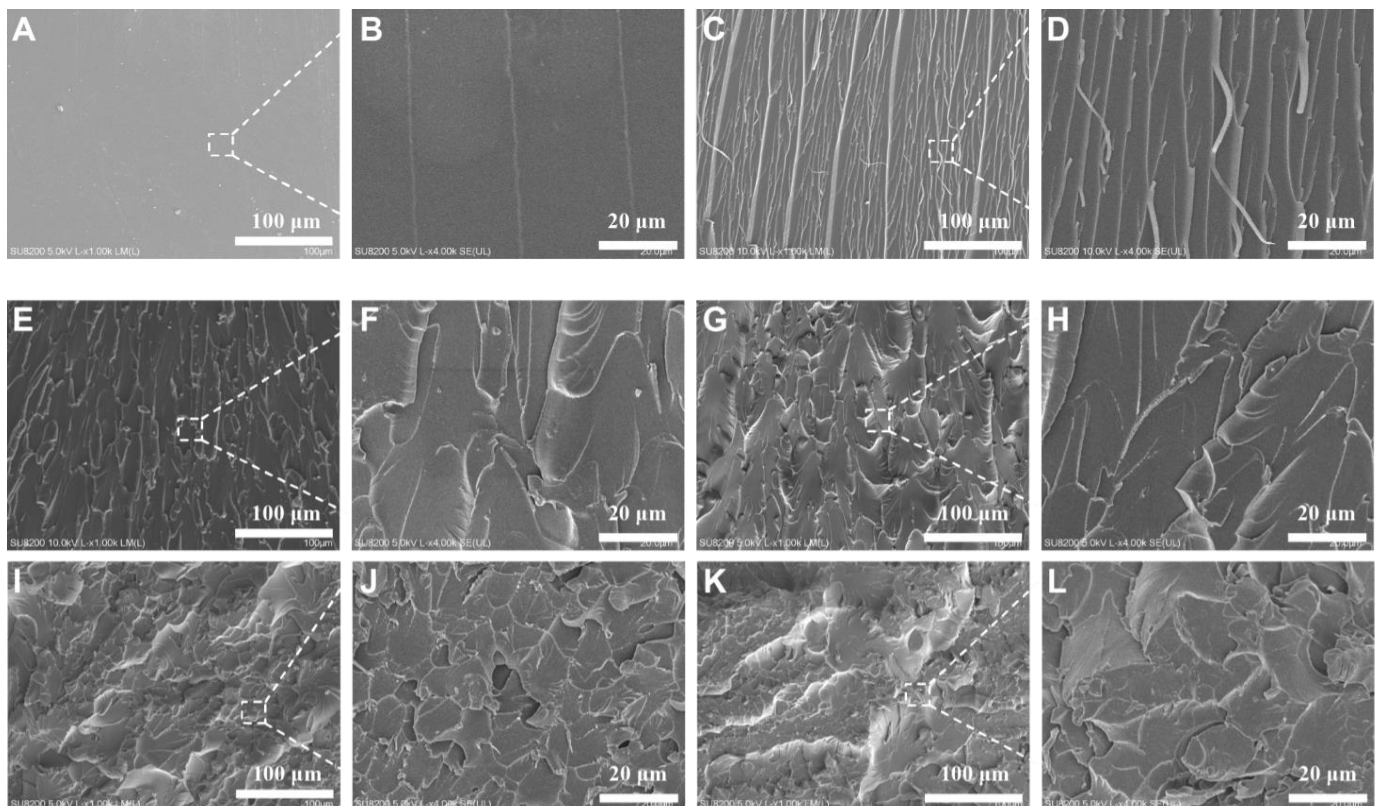

Figure 7. SEM micrographs of the blend for impact fractures ((**A**,**B**) E51, (**C**,**D**) 3 phr, (**E**,**F**) 5 phr, (**G**,**H**) 10 phr, (**I**,**J**) 15 phr, (**K**,**L**) 20 phr).

Figure 8 shows the SEM of the 10 phr-PPENK/E51 blend before and after fracture, as well as a schematic diagram of crack extension. The pure E51 system had a high cross-linking density, while the cross-linked network had poor resistance to crack propagation, which was prone to crack and brittle fracture. The introduction of PPENK increased the resistance of PPENK/E51 blends to crack propagation. In Figure 8B, the crack gradually spreads from the impact point to the surroundings. It was continuously deflected, increasing the energy consumption of crack propagation [39,40]. Therefore, it could be speculated that PPENK toughens E51 mainly through crack deflection, which was consistent with the previous conclusion.

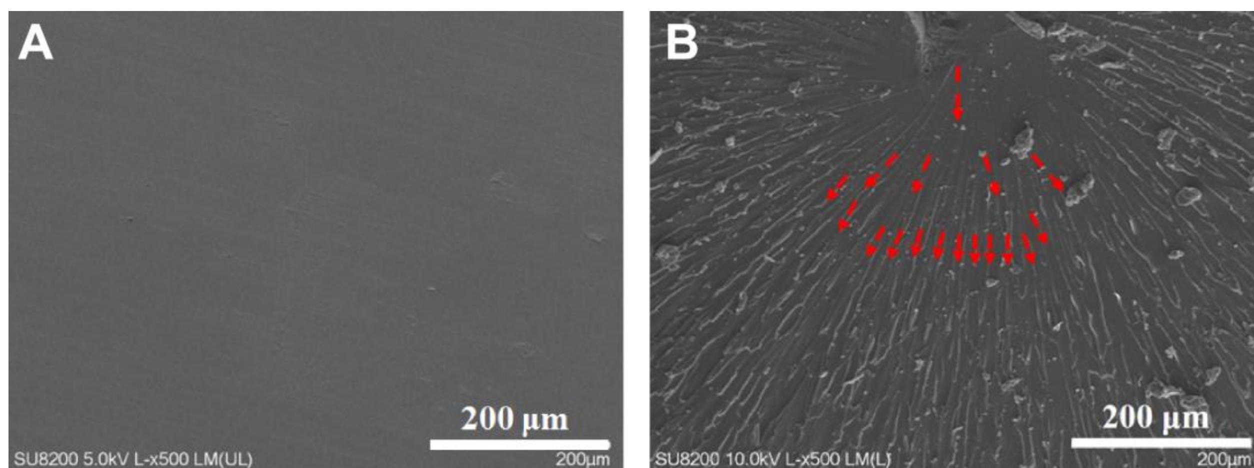

Figure 8. SEM micrographs and crack propagation path of 10 phr-PPENK/E51 blend ((**A**) Before fracture, (**B**) After fracture).

3.6. Low−Temperature Properties

Low−temperature performance was one of the important physical properties of epoxy resin. In this section, the evolution law of mechanical properties of epoxy resins in the liquid-oxygen temperature range was studied, and the corresponding results are shown in Figure 9. In the low-temperature environment (−183 °C), the epoxy resin also bears the internal shrinkage force while the external force is applied. In addition, the degree of molecular orientation of E51 resin increased results in smaller free volumes and stress concentration aggravated, making it easier to form cracks and brittle fractures when impacted [41]. Therefore, its impact strength at low-temperature values was generally low (Figure 9A). When PPENK was introduced, the polar molecules of PPENK made it compatible with E51, forming a uniform interpenetrating structure, which expanded the distance between E51 molecules and increased the activity space of E51 molecules, causing the PPENK/E51 blends to have some flexibility at low temperature (−183 °C). In addition, the PPENK molecule contained a twisted, non-coplanar bis-diazapine structure [42,43]. This unique structure enabled the molecular chain to maintain a sizeable free volume even at low temperatures, and its toughness can be well genetically preserved. The above two worked together to make the blend keep good impact toughness even at low-temperature (−183 °C).

The flexural properties of PPENK/E51 blends were also significantly affected in low-temperature environments. Based on Figure 9B, the flexural strength and modulus of pure E51 and PPENK/E51 blends had significantly improved. When the content of PPENK was 15 phr, the maximum bending strength was 230 MPa, which was 45.6% and 88.5% higher than pure E51 at low-temperature (−183 °C) and room temperature, respectively. In low-temperature environments, the molecular chains of E51 and PPENK shrink and become rigid, and the overall stiffness of the system increases [44,45]. In addition, reducing the intermolecular distance increased the intermolecular force, increasing the frictional resistance between the molecules, so the load at the time of failure was larger. Therefore, the PPENK/E51 blend’s flexural strength and modulus were increased.

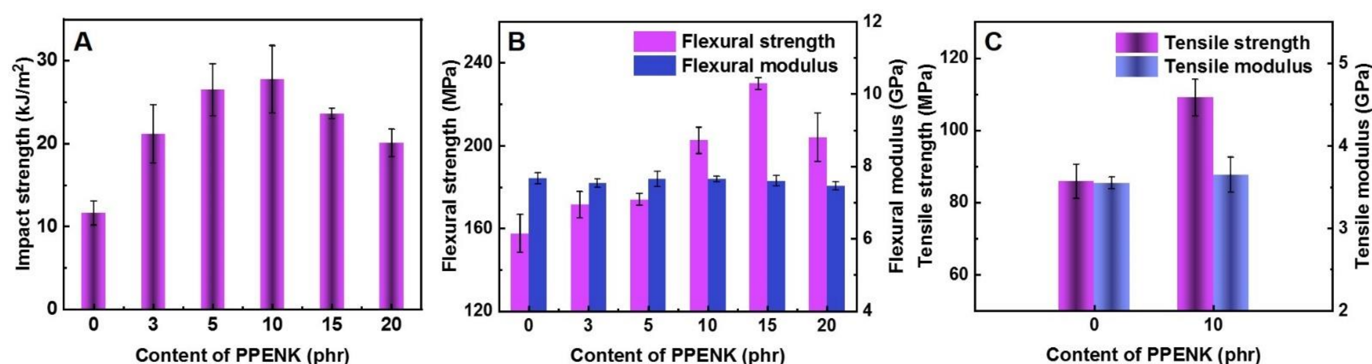

Figure 9. Mechanical properties of cured PPENK/E51 blends at low-temperature (−183 °C): (**A**) Impact strength, (**B**) flexural properties, (**C**) tensile properties.

Similar to the flexural properties at low-temperature (−183 °C), the PPENK/E51 blend's tensile strength and modulus were improved compared to those at room temperature. Figure 9C shows the low-temperature tensile strength of PPENK/E51 blends. The 10 phr-PPENK/E51 blend's tensile strength was 109 MPa, 33.8% higher than at room temperature (80 MPa, Figure 6B). At the low temperature (−183 °C), the molecular chains of the blends were frozen, and the resin fluidity was reduced, resulting in tensile strength and modulus increase [46].

Figure 10 shows the blend's SEM image after the low-temperature (−183 °C) impact fracture. From Figure 10, the 10 phr−PPENK/E51 blend's fracture surface was rougher and had more microcracks than the pure E51 resin. On the one hand, PPENK and E51 blended uniformly during molding. As a stress concentration point, PPENK could induce more microcracks to absorb energy and delay the propagation of cracks when stressed. On the other hand, PPENK riveted the damage by bridging it in the E51 matrix to restrain crack propagation. Combining these two effects increased the impact toughness of the 10 phr-PPENK/E51 blend.

3.7. Thermal Stability

Thermogravimetric analysis (TGA) was used to test the thermal stability of the cured blend systems [47,48], and the thermal weight loss curves were displayed in Figure 11. In addition, the blend's 5% thermal weight loss temperature ($T_{d5\%}$) and maximum thermal weight loss temperature (T_{dmax}) are shown in Table 4. From Table 4, the PPENK/E51 blends all had a $T_{d5\%}$ above 390 °C and a T_{dmax} of around 420 °C. Compared with pure E51, these values did not change much, and some increased. Interestingly, the residual mass at 800 °C increased with increasing PPENK content, which was attributed to the excellent thermal properties of PPENK (Table S3). Therefore, although the addition of PPENK led to a decrease in the crosslink density of E51, the good thermal properties of PPENK made up for this shortcoming, so PPENK/E51 still had good thermal stability.

Table 4. Thermal stability date of PPENK/E51 blends.

Blend Systems	$T_{d5\%}$ (°C)	T_{dmax} (°C)	Char Yield (%)
E51	392	417	8.35
3 phr−PPENK/E51	395	420	12.99
5 phr−PPENK/E51	391	421	14.95
10 phr−PPENK/E51	393	418	17.97
15 phr−PPENK/E51	390	417	17.19
20 phr−PPENK/E51	391	417	20.54

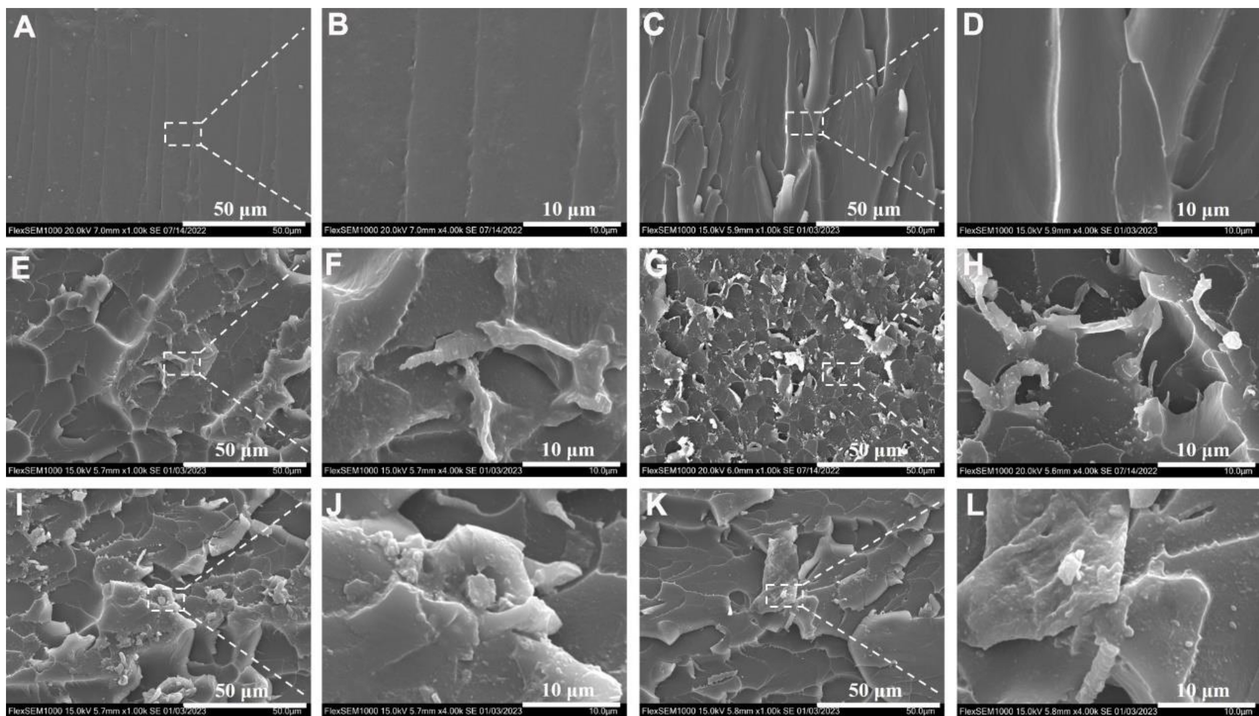

Figure 10. SEM micrographs of the low-temperature impact section of PPENK/E51 ((**A**,**B**) E51, (**C**,**D**) 3 phr, (**E**,**F**) 5 phr, (**G**,**H**) 10 phr, (**I**,**J**) 15 phr, (**K**,**L**) 20 phr).

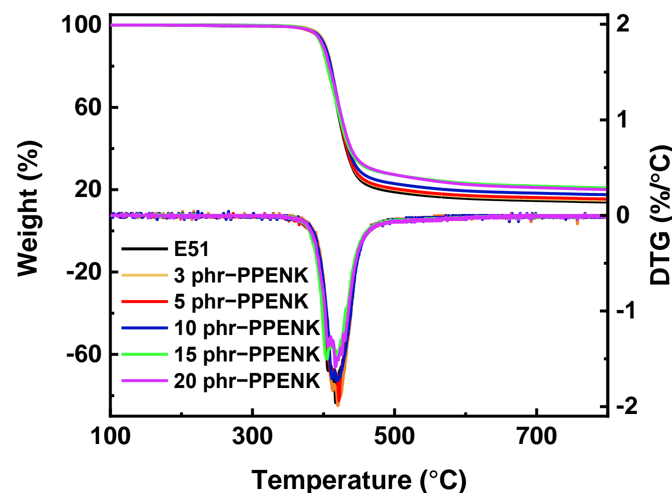

Figure 11. TGA curves of PPENK/E51 blends.

4. Conclusions

High-performance thermoplastic poly aryl ether PPENK was applied to modify the epoxy resin E51. With the addition of PPENK, the crosslink density of E51 was reduced. At the same time, the T_g of the blends was significantly increased (~50 °C). The blends had excellent mechanical and low−temperature properties (−183 °C). When the PPENK content was 10 phr, the impact strength of the blend was 131.0% higher than pure E51. When the PPENK content was 15 phr, the low−temperature flexural strength was 46.5% higher than pure E51. All in all, this research will provide a fresh perspective and theoretical support to improve epoxy resins' mechanical, thermal, and low-temperature properties.

Supplementary Materials: The following supporting information can be downloaded at: https://www.mdpi.com/article/10.3390/ma16072878/s1, Figure S1: Curves of PPENK/E51 blends curing

exothermic peak temperature and heating rate: A E51, B 10 phr-PPENK/E51. Figure S2: Fitting line of E51/DDS: A Kissinger method, B Ozawa method; Figure S3: Fitting line of 10%-PPENK/ E51/DDS: A Kissinger method, B Ozawa method; Figure S4: A DSC curves and B TGA curves of PPENK. Figure S5: A Typical tensile load–displacement curves, B Typical flexural load–displacement curves; Figure S6: Curing molds for PPENK/E51 blends; Table S1: Curing exothermic peak temperature of E51 at different heating rates. Table S2: Curing exothermic peak temperature of PPENK/E51 at different heating rates. Table S3: The crosslinking density of different blend systems. Table S4 DSC data and TGA data of PPENK; Table S5: The mechanical properties of blends at room temperature and ultra-low temperature.

Author Contributions: Conceptualization, B.W., G.Z., N.L. and X.F.; Formal analysis, Z.W. (Zaiyu Wang) and G.L.; Investigation, H.G. and B.W.; Resources, Z.W. (Zhihuan Weng); Data curation, C.L. and G.L.; Writing—original draft, H.G.; Writing—review & editing, H.G., S.Z. and Y.C.; Visualization, S.Z. and X.J.; Supervision, G.L., G.Z., X.J. and Y.C.; Funding acquisition, N.L.; Methodology, N.L. All authors have read and agreed to the published version of the manuscript.

Funding: This work was financially supported by the State Key Laboratory for Modification of Chemical Fibers and Polymer Materials, Donghua University (KF2002), the National Key Research and Development Program of China (2020YFB0311600), the Fundamental Research Funds for the Central Universities (DUT22GF402; DUT20TD114; DUT20LAB305, DUT22LAB605), Young Elite Scientists Sponsorship Program by CAST (2021QRNC001), the Key Laboratory Foundation of State Key Laboratory of Organic-Inorganic Composites (oic-201901005), and the National Science Foundation of China (U1837205; 91860204; 52203081).

Institutional Review Board Statement: Not applicable.

Informed Consent Statement: Not applicable.

Data Availability Statement: Not applicable.

Conflicts of Interest: The authors declare no conflict of interest.

References

1. Lian, Q.; Chen, H.; Luo, Y.; Li, Y.; Cheng, J.; Liu, Y. Toughening mechanism based on the physical entanglement of branched epoxy resin in the non-phase-separated inhomogeneous crosslinking network: An experimental and molecular dynamics simulation study. *Polymer* **2022**, *247*, 124754. [CrossRef]
2. Tian, J.; Li, C.; Xian, G. Reciprocating friction and wear performances of nanometer sized-TiO_2 filled epoxy composites. *Polym. Compos.* **2021**, *42*, 2061–2072. [CrossRef]
3. Gholinezhad, F.; Golhosseini, R.; Moini Jazani, O. Synthesis, characterization, and properties of silicone grafted epoxy/acrylonitrile butadiene styrene/graphene oxide nanocomposite with high adhesion strength and thermal stability. *Polym. Compos.* **2022**, *43*, 1665–1684. [CrossRef]
4. Tangthana-umrung, K.; Zhang, X.; Gresil, M. Synergistic toughening on hybrid epoxy nanocomposites by introducing engineering thermoplastic and carbon-based nanomaterials. *Polymer* **2022**, *245*, 124703. [CrossRef]
5. Mousavi, S.R.; Estaji, S.; Paydayesh, A.; Arjmand, M.; Jafari, S.H.; Nouranian, S.; Khonakdar, H.A. A review of recent progress in improving the fracture toughness of epoxy-based composites using carbonaceous nanofillers. *Polym. Compos.* **2022**, *43*, 1871–1886. [CrossRef]
6. Jin, Q.; Misasi, J.M.; Wiggins, J.S.; Morgan, S.E. Simultaneous reinforcement and toughness improvement in an aromatic epoxy network with an aliphatic hyperbranched epoxy modifier. *Polymer* **2015**, *73*, 174–182. [CrossRef]
7. Shen, Y.B.; Wang, B.L.; Li, D.; Xu, X.R.; Liu, Y.Y.; Huang, Y.D.; Hu, Z. Toughening shape-memory epoxy resins via sacrificial hydrogen bonds. *Polym. Chem.* **2022**, *13*, 1130–1139. [CrossRef]
8. Su, W.C.; Tsai, F.C.; Huang, C.F.; Dai, L.Z.; Kuo, S.W. Flexible Epoxy Resins Formed by Blending with the Diblock Copolymer PEO-b-PCL and Using a Hydrogen-Bonding Benzoxazine as the Curing Agent. *Polymers* **2019**, *11*, 11020201. [CrossRef]
9. Yi, J.; Li, S.H.; Xia, J.L.; Li, M.; Ding, H.Y.; Xu, L.N.; Yang, X.H. Preparation and Properties of Polyether Aliphatic Polymerized Amide as a Vegetable Oil-Based Epoxy Curing Agent. *ACS Omega* **2019**, *4*, 6238–6244. [CrossRef]
10. Akbolat, M.C.; Katnam, K.B.; Soutis, C.; Potluri, P.; Sprenger, S.; Taylor, J. On mode-I and mode-II interlaminar crack migration and R-curves in carbon/epoxy laminates with hybrid toughening via core-shell rubber particles and thermoplastic micro-fibre veils. *Compos. Part B Eng.* **2022**, *238*, 109900. [CrossRef]
11. Mousavi, S.R.; Estaji, S.; Javidi, M.R.; Paydayesh, A.; Khonakdar, H.A.; Arjmand, M.; Rostami, E.; Jafari, S.H. Toughening of epoxy resin systems using core-shell rubber particles: A literature review. *J. Mater Sci.* **2021**, *56*, 18345–18367. [CrossRef]
12. Li, L.; Peng, W.; Liu, L.; Zheng, S. Toughening of epoxy by nanostructures with ABA triblock copolymers: An influence of organosilicon modification of block copolymer. *Polym. Eng. Sci.* **2022**, *62*, 392–404. [CrossRef]

13. Zhao, X.L.; Hou, G.X.; Yu, S.W.; Wang, M.Y. Preparation of HNTs-d-GO hybrid nanoparticles for gallic acid epoxy composites with improved thermal and mechanical properties. *Polym. Compos.* **2022**, *43*, 5133–5144. [CrossRef]
14. Wang, T.-T.; Huang, P.; Li, Y.-Q.; He, N.; Fu, S.-Y. Epoxy nanocomposites significantly toughened by both poly(sulfone) and graphene oxide. *Compos. Commun* **2019**, *14*, 55–60. [CrossRef]
15. Liu, Z.; Yuan, L.; Liang, G.Z.; Gu, A.J. Tough epoxy/cyanate ester resins with improved thermal stability, lower dielectric constant and loss based on unique hyperbranched polysiloxane liquid crystalline. *Polym. Advan. Technol.* **2015**, *26*, 1608–1618. [CrossRef]
16. Sinh, L.H.; Son, B.T.; Trung, N.N.; Lim, D.G.; Shin, S.; Bae, J.Y. Improvements in thermal, mechanical, and dielectric properties of epoxy resin by chemical modification with a novel amino-terminated liquid-crystalline copoly(ester amide). *React. Funct. Polym.* **2012**, *72*, 542–548. [CrossRef]
17. Punchaipetch, P.; Ambrogi, V.; Giamberini, M.; Brostow, W.; Carfagna, C.; D'Souza, N.A. Epoxy+liquid crystalline epoxy coreacted networks: II. Mechanical properties. *Polymer* **2002**, *43*, 839–848. [CrossRef]
18. Van Velthem, P.; Ballout, W.; Horion, J.; Janssens, Y.A.; Destoop, V.; Pardoen, T.; Bailly, C. Morphology and fracture properties of toughened highly crosslinked epoxy composites: A comparative study between high and low T-g tougheners. *Compos. Part B Eng.* **2016**, *101*, 14–20. [CrossRef]
19. Zhou, J.; Zhang, C.; Cheng, C.; Wang, M.; Yang, Z.; Yang, Y.; Yang, H.; Yu, M. Synergetic Improvement of Interlaminar Fracture Toughness in Carbon Fiber/Epoxy Composites Interleaved with PES/PEK-C Hybrid Nanofiber Veils. *Adv. Fiber Mater.* **2022**, *4*, 1081–1093. [CrossRef]
20. Ma, T.Y.; Sun, Y.K.; Yao, J.W. Influence of carbon nanotubes/polyetherketone-cardo interlayer structure on mode II interlaminar fracture toughness of the interleaved carbon fiber reinforced epoxy composites. *J. Appl. Polym. Sci.* **2022**, *139*, e52671. [CrossRef]
21. Daelemans, L.; van der Heijden, S.; De Baere, I.; Muhammad, I.; Van Paepegem, W.; Rahier, H.; De Clerck, K. Bisphenol A based polyester binder as an effective interlaminar toughener. *Compos. Part B Eng.* **2015**, *80*, 145–153. [CrossRef]
22. Wang, J.F.; Zhang, X.H.; Jiang, L.; Qiao, J.L. Advances in toughened polymer materials by structured rubber particles. *Prog. Polym. Sci.* **2019**, *98*, 101160. [CrossRef]
23. Goyat, M.S.; Hooda, A.; Gupta, T.K.; Kumar, K.; Halder, S.; Ghosh, P.K.; Dehiya, B.S. Role of non-functionalized oxide nanoparticles on mechanical properties and toughening mechanisms of epoxy nanocomposites. *Ceram. Int.* **2021**, *47*, 22316–22344. [CrossRef]
24. Zhao, L.W.; Li, H.F.; Qiao, Y.J.; Bai, X.F.; Wang, D.Z.; Qu, C.Y.; Xiao, W.B.; Liu, Y.; Zhang, J. Accelerated-curing epoxy structural film adhesive for bonding lightweight honeycomb sandwich structures. *J. Appl. Polym. Sci.* **2023**, *140*, 53458. [CrossRef]
25. Bhudolia, S.K.; Gohel, G.; Vasudevan, D.; Leong, K.F.; Gerard, P. On the Mode II fracture toughness, failure, and toughening mechanisms of wholly thermoplastic composites with ultra-lightweight thermoplastic fabrics and innovative Elium (R) resin. *Compos. Part A Appl. Sci. Manuf.* **2022**, *161*, 107115. [CrossRef]
26. Karthikeyan, L.; Robert, T.M.; Mathew, D.; Desakumaran Suma, D.; Thomas, D. Novel epoxy resin adhesives toughened by functionalized poly (ether ether ketone) s. *Int. J. Adhes. Adhes.* **2021**, *106*, 102816. [CrossRef]
27. Rehman, M.M.; Shaker, K.; Nawab, Y. Effect of poly ether ether ketone particles on v-notched shear and drop weight impact behavior of carbon/epoxy composite. *Polym. Compos.* **2022**, *43*, 3219–3227. [CrossRef]
28. Zhang, Y.; Liu, C.; Jia, H.; Qiao, Y.; Dang, X.X.; Weng, Z.H.; Chen, Y.S.; Zou, J.X.; Jian, X.G. Effect of electrospun PPENK nanofiber loaded with ZnO nanowires on the mode II fracture toughness, flexural properties and ILSS of CF/poly (phthalazinone ether ketone) composites. *Compos. Part B Eng.* **2022**, *244*, 110172. [CrossRef]
29. Niu, Y.A.; Ma, Y.H.; Song, B.L.; Yang, L.; Wang, L.; Zheng, S.J.; Zhang, X. Design, synthesis, and water resistance properties of bis(4-maleimidephenyl) adamantane and hybrid resins. *J. Appl. Polym. Sci.* **2022**, *139*, 51692. [CrossRef]
30. Wang, B.; Li, N.; Bao, Q.G.; Liu, D.M.; Guo, H.J.; Li, G.Y.; Zheng, G.D.; Zhang, G.S.; Qiao, Y.; Weng, Z.H.; et al. Toughening and strengthening of low-temperature resistant epoxy resins by introducing high-performance thermoplastic resin with phthalazinone structure. *Polymer* **2023**, *266*, 125619. [CrossRef]
31. Liu, C.H.; Liu, W.Q.; He, S.; Jiang, C.; Xie, Y.K.; Yang, M.P.; Shi, H.Y.; Wang, Z.F. Highly exfoliated epoxy/clay nanocomposites filled with novel cationic fluorinated polyacrylate modified montmorillonite: Morphology and mechanical properties. *Polym. Compos.* **2019**, *40*, 4266–4280. [CrossRef]
32. Zong, L.; Li, J.; Liu, C.; Zu, Y.; Li, N.; Wang, J.; Jian, X. Polybenzoxazine thermosets with enhanced toughness via blending with phthalazinone-bearing thermal plastic copoly(aryl ether nitrile)s. *J. Appl. Polym. Sci.* **2019**, *137*, 48508. [CrossRef]
33. Sodeifian, G.; Ghaseminejad, S.; Yousefi, A.A. Preparation of polypropylene/short glass fiber composite as Fused Deposition Modeling (FDM) filament. *Results Phys.* **2019**, *12*, 205–222. [CrossRef]
34. Liu, J.; Wang, S.; Su, Q.; He, J.; Li, Y.; Xie, J.; Yi, G. Synthesis of a novel hyperbranched polyester with carboxyl end groups applied to UV-curable waterborne coating. *J. Coat. Technol. Res.* **2021**, *18*, 259–269. [CrossRef]
35. Chen, D.; Li, J.; Yuan, Y.; Gao, C.; Cui, Y.; Li, S.; Wang, H.; Peng, C.; Liu, X.; Wu, Z.; et al. A new strategy to improve the toughness of epoxy thermosets by introducing the thermoplastic epoxy. *Polymer* **2022**, *240*, 124518. [CrossRef]
36. Luo, X.; Liu, X.-F.; Ding, X.-M.; Chen, L.; Chen, S.-C.; Wang, Y.-Z. Effects of curing temperature on the structure and properties of epoxy resin-poly(ε-caprolactam) blends. *Polymer* **2021**, *228*, 123940. [CrossRef]
37. Ma, H.; Aravand, M.A.; Falzon, B.G. Phase morphology and mechanical properties of polyetherimide modified epoxy resins: A comparative study. *Polymer* **2019**, *179*, 121640. [CrossRef]

38. Xiao, L.; Huang, J.; Wang, Y.; Chen, J.; Liu, Z.; Nie, X. Tung Oil-Based Modifier Toughening Epoxy Resin by Sacrificial Bonds. *ACS Sustain. Chem. Eng.* **2019**, *7*, 17344–17353. [CrossRef]
39. Voleppe, Q.; Ballout, W.; Van Velthem, P.; Bailly, C.; Pardoen, T. Enhanced fracture resistance of thermoset/thermoplastic interfaces through crack trapping in a morphology gradient. *Polymer* **2021**, *218*, 123497. [CrossRef]
40. Muñoz, B.K.; del Bosque, A.; Sánchez, M.; Utrilla, V.; Prolongo, S.G.; Prolongo, M.G.; Ureña, A. Epoxy resin systems modified with ionic liquids and ceramic nanoparticles as structural composites for multifunctional applications. *Polymer* **2021**, *214*, 123233. [CrossRef]
41. Hussein, A.; Sarkar, S.; Lee, K.; Kim, B. Cryogenic fracture behavior of epoxy reinforced by a novel graphene oxide/poly(p-phenylenediamine) hybrid. *Compos. Part B Eng.* **2017**, *129*, 133–142. [CrossRef]
42. Liu, C.; Qiao, Y.; Jia, H.; Li, N.; Chen, Y.S.; Jian, X.G. Improved mechanical properties of basalt fiber/phthalonitrile composites modified by thermoplastic Poly(phthalazinone ether nitrile)s. *Polymer* **2021**, *228*, 123974. [CrossRef]
43. Li, Y.Z.; Liu, C.D.; Liu, W.T.; Cheng, X.T.; Zhang, A.; Zhang, S.H.; Liu, C.; Li, N.; Jian, X.G. Apatite Formation Induced by Chitosan/Gelatin Hydrogel Coating Anchored on Poly(aryl ether nitrile ketone) Substrates to Promote Osteoblastic Differentiation. *Macromol. Biosci.* **2021**, *21*, 2100262. [CrossRef] [PubMed]
44. Takeda, T.; Shindo, Y.; Watanabe, S.; Narita, F. Three-dimensional stress analysis of cracked satin woven carbon fiber reinforced/polymer composites under tension at cryogenic temperatures. *Cryogenics* **2012**, *52*, 784–792. [CrossRef]
45. Yan, M.L.; Jiao, W.C.; Li, J.; Huang, Y.F.; Chu, Z.M.; Chen, X.D.; Shen, F.; Wang, Y.; Wang, R.G.; He, X.D. Enhancement of the cryogenic-interfacial-strength of carbon fiber composites by chemical grafting of graphene oxide/attapulgite onT300. *Polym. Compos.* **2020**, *41*, 5072–5081. [CrossRef]
46. Chang, W.; Rose, L.R.F.; Islam, M.S.; Wu, S.; Peng, S.; Huang, F.; Kinloch, A.J.; Wang, C.H. Strengthening and toughening epoxy polymer at cryogenic temperature using cupric oxide nanorods. *Compos. Sci. Technol.* **2021**, *208*, 108762. [CrossRef]
47. Chen, Y.; Wu, L.; Li, B.-G. Poly(1,5-pentylene-co-2,2,4,4-tetramethyl cyclobutylene terephthalate) copolyesters with high Tg and improved ductility and thermal stability. *Polymer* **2021**, *232*, 124152. [CrossRef]
48. Xu, C.-A.; Qu, Z.; Meng, H.; Chen, B.; Wu, X.; Cui, X.; Wang, K.; Wu, K.; Shi, J.; Lu, M. Effect of polydopamine-modified multi-walled carbon nanotubes on the thermal stability and conductivity of UV-curable polyurethane/polysiloxane pressure-sensitive adhesives. *Polymer* **2021**, *223*, 123615. [CrossRef]

Disclaimer/Publisher's Note: The statements, opinions and data contained in all publications are solely those of the individual author(s) and contributor(s) and not of MDPI and/or the editor(s). MDPI and/or the editor(s) disclaim responsibility for any injury to people or property resulting from any ideas, methods, instructions or products referred to in the content.